Phonon instability and pressure-induced isostructural semiconductor-semimetal transition of monoclinic VO_{2}

Huabing He, Heng Gao, Wei Wu, Shixun Cao, Jiawang Hong, Dehong Yu, Guochu Deng, Yanfeng Gao, Peihong Zhang, Hongjie Luo, and Wei Ren

Phys. Rev. B **94**, 205127 — Published 16 November 2016

DOI: 10.1103/PhysRevB.94.205127

Phonon instability and pressure-induced isostructural semiconductor-semimetal transition of monoclinic VO_2

Huabing He,[1] Heng Gao,[1] Wei Wu,[1] Shixun Cao, [1,2] Jiawang Hong,[3] Dehong Yu[4], Guochu Deng[4], Yanfeng Gao,[2,6] Peihong Zhang,[5,1] Hongjie Luo,[2,6] and Wei Ren[1,2]

[1]International Centre for Quantum and Molecular Structures,
Physics Department, Shanghai University, Shanghai 200444, China
[2] Materials Genome Institute and Shanghai Key Laboratory of High Temperature Superconductors, Shanghai University, Shanghai 200444, China
[3]School of Aerospace Engineering, and Institute of Advanced Structure Technology, Beijing Institute of Technology, Beijing 100081, China
[4]Bragg Institute, Australian Nuclear Science and Technology Organization,
New Illawarra Road, Lucas Heights NSW-2234 Australia
[5]Department of Physics, University at Buffalo, State University of New York,
Buffalo, New York 14260, USA
[6]School of Materials Science and Engineering, Shanghai University, 99
Shangda Road, Shanghai 200444, China

ABSTRACT:

Recent experiments have revealed an intriguing pressure-induced isostructural transition of the low temperature monoclinic VO_2 and hinted to the existence of a new metallization mechanism in this system. The physics behind this isostructural phase transition and the metallization remains unresolved. In this work, we show that the isostructural transition is a result of pressure-induced instability of a phonon mode that relates to a $CaCl_2$-type of rotation of the oxygen octahedra which alleviates, but does not completely remove, the dimerization and zigzagging arrangement of V atoms in the M1 phase. This phonon mode shows an increasing softening with pressure, ultimately leading to an isostructural phase transition characterized by the degree of the rotation of the oxygen octahedra. We also find that this phase transition is accompanied by an anisotropic compression, in excellent agreement with experiments. More interestingly, in addition to the experimentally identified M1' phase, we find a closely related M1" phase which is nearly degenerate with the M1' phase. Unlike the M1' phase which has a nearly pressure-independent electronic band gap, the gap of the M1" drops quickly at high pressures and vanishes at a theoretical pressure of about 40 GPa.

I. INTRODUCTION

Vanadium dioxide (VO_2) is the most widely studied thermochromic material in the smart window technology [1, 2], as well as in electronic and optical applications for sensing and switching [3]. It undergoes a first-order phase transition [4] from a low-temperature insulating monoclinic (M1) structure (space group No. 14, $P2_1/c$, infrared transparent) to a metallic tetragonal rutile (R) structure (space group No. 136, $P4_2/mnm$, infrared reflecting) at 340K. Later it was shown that the metal-insulator transition (MIT) in VO_2 can be triggered not only by temperature, but also by strain [5, 6], terahertz (THz) wave [7, 8], electric gating [9, 10], and ultrafast photoexcitations

[8, 11-18]. The fundamental mechanism and practical applications of the MIT in VO_2 have inspired extensive investigations [19-24]. Although the basic mechanism of the metal-insulator transition in VO_2 was explained by Goodenough [25], a complete understanding of the physics behind the MIT remains a subject of constant debate. Various theories have been proposed, including the Mott transition with electron correlation [20, 26, 27], the Peierls structural transition mechanism [28-31], orbital selectivity [32-34] cooperative Mott-Peierls mechanism, and the effects of phonon entropy [35]. Goodenough [25] proposed a vivid picture to describe the M1-R transition, in which the $3d$ orbitals of V atoms split into lower t_{2g} and higher e_g^{σ} orbitals, with the t_{2g} further splits into an e_g^{π} doublet and an a_{1g} singlet due to a tetragonal crystal field. It is generally agreed that the splitting of a_{1g} to bonding and antibonding orbitals ($d_{//}$ and $d_{//*}$) is responsible for the band gap opening in M1 phase.

Under normal condition, the MIT is accompanied by a first-order structural phase transition. However, recent experiments on pressure-induced isostructural insulator-metal transition hint to a different metallization mechanism. The properties of VO_2 under high pressures have been investigated by Arcangeletti *et al.* [36] using Raman spectroscopy combined with infrared transmission and reflectivity measurements. They concluded that a new room temperature metallic VO_2 phase with a monoclinic structure exist in high pressure regime (P > 10 GPa), and that this pressure-induced metallization does not require the breaking of V-V dimers, suggesting that Peierls distortions exist in the new metallic phase. Marini et al. [37] also believed that VO_2 shows two distinct regimes at low pressure (insulator) and high pressure (metal) from their Raman and infrared data. Later, Mitrano *et al.* [38] observed a remarkable anisotropic compression (in the *b-c* plane) above 12 GPa in pure and Cr-doped VO_2, revealing an isostructural transition and that preserves the M1 symmetry ($P2_1/c$) across a large range of pressure.

More recently, Zhang *et al.* reported a semiconductor-to-semiconductor transition in the polycrystalline M1 phase at 10.4 GPa by measuring the temperature-dependent resistivity [39], and the anomalous electrical behavior was observed to be accompanied with an isostructural phase transition. Bai *et al.* [40] investigated VO_2 at room temperature and a higher temperature (383 K) using synchrotron X-ray diffraction, electrical resistivity, and Raman spectroscopy measurements, and they confirmed anisotropic compression behaviors for both the R and M1 phases. An isostructural phase transition of the M1 phase starting at about 13.0 GPa was observed, resulting in a distorted M1 phase (called M1'). However, pressure-induced metallization was not observed in the M1' phase below 34.3 GPa. Instead, a gradual reduction of the band gap with increasing pressure was observed. However, their band structure calculations did not reproduce the observed pressure-dependent band gap. Bai *et al.* [40] also showed that, upon further compression, both high pressure metallic and insulating phases transform into a new metallic phase X. Figure 1 shows the tentative temperature-pressure phase diagram of VO_2 based on available experimental results.

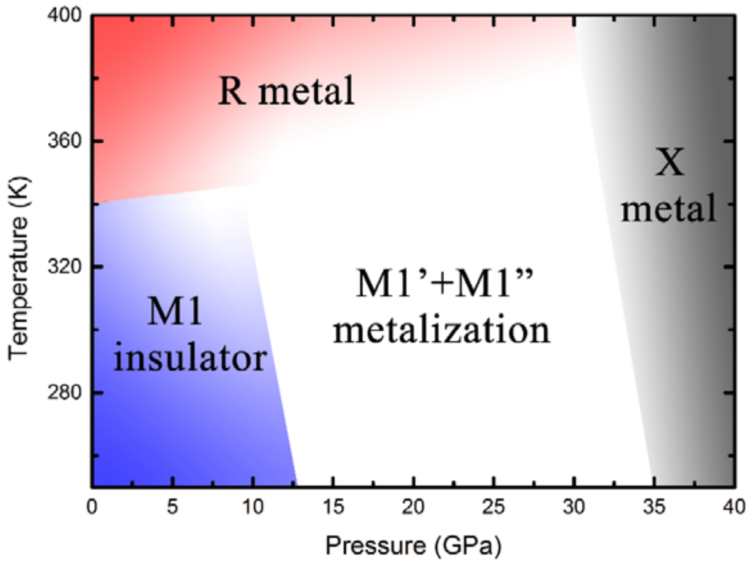

Figure 1. Tentative pressure-temperature phase diagram of VO_2.

In this work, detailed first-principles calculations and analyses of the pressure effects on the electronic, phonon, and structural properties of VO_2 have been carried out to understand the pressure-induced isostructural phase transition and the associated band gap reduction and metallization mechanism. We find that the isostructural transition is a result of pressure-induced instability of a phonon mode that relates to the rotation of the oxygen octahedra. This phonon mode shows an increasing softening with pressure, ultimately leading to an isostructural phase transition characterized by the degree of the rotation of the oxygen octahedra.

Besides the earlier identified semiconducting M1' phase, a new distorted phase M1" is predicted in our work here. This new phase is closely related to the M1' phase but exhibits a rather different pressure-dependent band gap behavior. Unlike the M1' phase which shows a nearly pressure-independent band gap, the band gap of the M1" phase decreases continuously with increasing pressure, eventually transforming into a semimetal at around 40GPa. The pressure-induced gap reduction and metallization in the M1" is a continuous process which is attributed to the de-dimerization and de-zigzagging of the V chains with increasing pressure.

II. COMPUTATIONAL METHODS

The density-functional-theory (DFT) calculations were performed using the plane-wave projector-augmented wave method [41] as implemented in the Vienna Ab initio Simulation Package (VASP) [42] using the Perdew-Burke-Ernzerhof (PBE) functional [43] within the generalized gradient approximation (GGA). The geometric structure optimization was performed using the conjugated-gradient minimization scheme until the maximum residual force on each atom was less than 0.01 eV/Å. A cutoff of 600 eV for the plane-wave expansion was used in our calculations, and the total energies were converged to 10^{-6} eV. The Brillouin zone integration is sampled with a 9×9×9 Monkhorst-Pack grid. The band gap is calculated with GGA+U method [44] (with an effective $U = 2.65$ eV). The value of U is chosen to obtain an experimental gap [45] of the M1 phase at zero pressure. This value is also close to that calculated from a constrained random phase approximation method [46]. The phonon dispersions were computed based on the supercell approach using the PHONOPY code [47] with 2×2×2 supercells for the M1, M1' and M1" structures.

Before we proceed to present the main results, we would like to clarify a few issues that are often raised in the DFT studies of VO_2 regarding the correlation effects and the choice of energy functionals. There is a long history of debate on the role correlation plays in determining the electronic properties of VO_2, in particular, in the development of an insulating gap in the M1 phase. Granted, correlation effects are important in VO_2. However, we believe that the V-V dimerization plays a pivotal role in the band gap formation. In other words, it is the Peierls-like pairing distortion that is mainly responsible for the development of an insulating gap in this system, and this effect can be well described within the GGA [11]. Although it has been shown that the HSE hybrid functional can successfully reproduce the band gap for the M1 phase VO_2 [21], it was pointed out in a recent paper [32] that the HSE functional incorrectly predicts an antiferromagnetic ground state for all three phases (namely, M1, M2, and R) of VO_2.

Thus the choice of using DFT+U over more computationally demanding hybrid functionals is a result of several considerations. First, as far as energetics is concerned, the HSE functional has no advantages over conventional DFT or DFT+U functionals. We believe that the calculated relative energetics and structural properties within DFT+U are reliable for addressing the pressure-induced phase transition in this system. Second, if the band gap is of primary interest, then DFT+U can predict the band gap equally well at a greatly reduced computational cost. Third, performing extensive structural optimization using the HSE functional for various pressures and phases is extremely expensive computationally. In particular, phonon calculations using HSE functionals for many structures are prohibitively time-consuming.

We should also mention that the DFT+U approach has been used by several groups to study the electronic and structural properties of VO_2 [11, 32, 34, 35, 40]. Although the DFT+U approach was originally proposed for better treating correlated magnetic insulators, the idea of applying an on-site Coulomb U to DFT calculations for materials containing localized d electrons as a means to reduce the self-interaction among d electrons has been extended to the study of nonmagnetic semiconductors as well [48, 49].

III. RESULTS AND DISCUSSION

A. Pressure-induced phonon softening and structural instability

The pressure-induced isostructural phase transition observed in this system suggests the existence of a symmetry-preserving unstable phonon mode. Therefore, we first carry out structural optimization of the M1 phase under various pressures, followed by phonon calculations.

Figure 2(a) shows the low energy part of the phonon dispersion of the M1 phase calculated at various pressures. Full phonon structures are presented in Supplemental

Materials (Figures S1). The softening of a Γ phonon mode (indicated by black arrows) is clearly seen. The energy of this phonon mode drops quickly with increasing pressure and becomes imaginary at around 28 GPa. Upon close examination, we find that this phonon mode corresponds to the $CaCl_2$-type of rotation of the oxygen octahedron (with minor V components) as shown in Figure 2(b). The oxygen octahedron rotation is usually related to the dynamic stability of various oxide compounds [50, 51]. We mention that this oxygen octahedron rotation is also known to be responsible for the observed phase transition of the high-temperature R phase: The R phase deforms to a $CaCl_2$-type phase (R', Pnnm, space group No. 58) at around 13 GPa [40]. This R' phase is quite commonly seen in many other metal dioxides (e.g. stishovite SiO_2, GeO_2, SnO_2, PbO_2, etc.) [52].

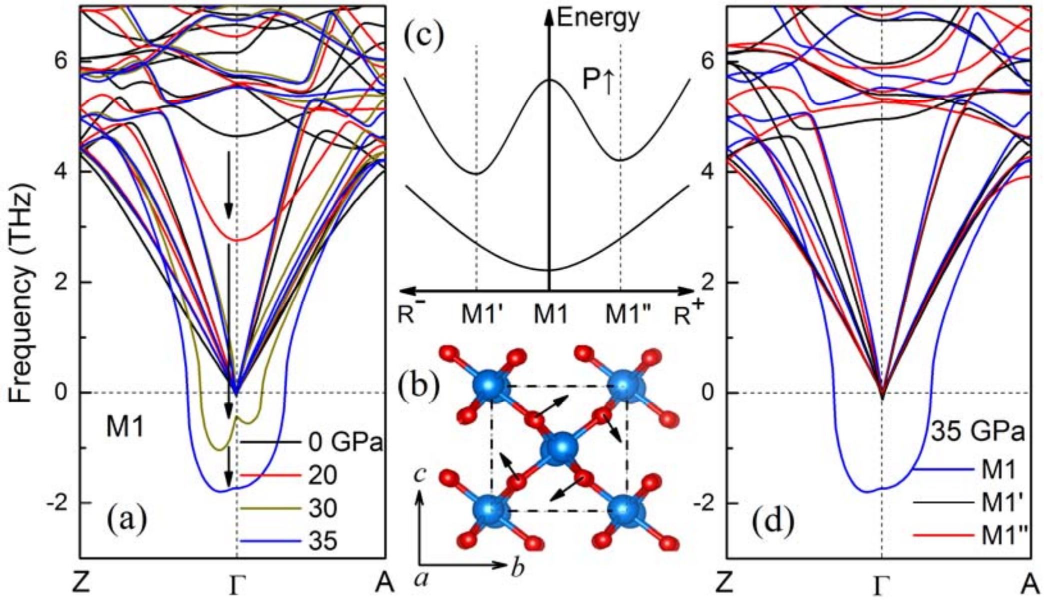

Figure 2. (a) Phonon structure of the M1 phase calculated at various pressures showing the pressure-induced softening of a zone center phonon mode. (b) Phonon polarization vector of the soft phonon, showing that this phonon mode is related to the rotation of the oxygen octahedron. Oxygen atoms are colored red and V atoms in blue. (c) Schematics of the development of a double well structure with increasing pressure associated with the rotation of oxygen octahedron. (d) Phonon structure of M1 (blue), M1' (black), and M1" (red) phases calculated at 35 GPa, showing the dynamical stability of the M1' and M1" phases.

When the $CaCl_2$-type rotation is introduced in the M1 phase VO_2, the resulting phase still holds the same isostructural space group ($P2_1/c$, space group No. 14). However, the clockwise (M1") and anticlockwise (M1') rotations (viewed along the *a* axis) are not equivalent, leading to two different structures with distinct electronic properties under high pressure as we will discuss later. Figure 2(c) illustrates schematically the development of a double-well structure with respect to the oxygen octahedron rotation with increasing pressure, giving rise to two local minima. We would like to mention the isostructural transition may occur before the energy of this phonon mode becomes imaginary. Figure 2(d) shows the phonon dispersion of the M1 (blue), M1’ (black), and M1” (red) at 35 GPa. Not surprisingly, the rotational distortions in both the M1’ and M1” remove the unstable phonon mode, thus restoring the structural stability. These results clearly suggest that the $CaCl_2$-type of oxygen rotational instability is responsible for the observed pressure-induced isostructural phase transition.

B. Anisotropic compression behavior

Experimentally, the onset of the isostructural transition is accompanied by an anisotropic compression behavior of the *b* and *c* lattice constants. This is not unusual as the oxygen rotational distortions are primarily in the *b*-*c* plane. Figure 3 shows the calculated evolution of the lattice parameters of the M1’ and M1” phases starting from 10 GPa. At lower pressures, the M1’ and M1” phases both converge to M1. Lattice constant *a* shows a linear dependence with increasing pressure. Lattice constants *b* and *c*, on the other hand, show a multitude of abnormal behaviors. First, for the M1’ phase, we observe a small jump in lattice constants *b* and *c* at about 13 GPa, which coincides with the development of the $CaCl_2$-type of rotation of oxygen octahedral as mentioned earlier. It is tempting to associate this onset of oxygen rotation with the onset of isostructural transition observed experimentally. However, one must be cautious since current theory might not be able to predict precisely the transition pressure. The *b* and *c* parameters then evolve smoothly with pressure until the pressure reaches about 19 GPa at which point lattice parameter *b* of the M1’ phase starts to decrease significantly. Lattice parameter *c* shows a small negative differential compressibility starting at theoretical pressure of 19 GPa. Overall, lattice parameter *c* of the M1’ phase is less sensitive to pressure. These results are in qualitative agreement with experiments. [38, 40] Lattice constants *b* and *c* for the M1” phase shows opposite trends as the clockwise oxygen rotation favors a shorter *c* lattice constant and a longer *b* lattice constant.

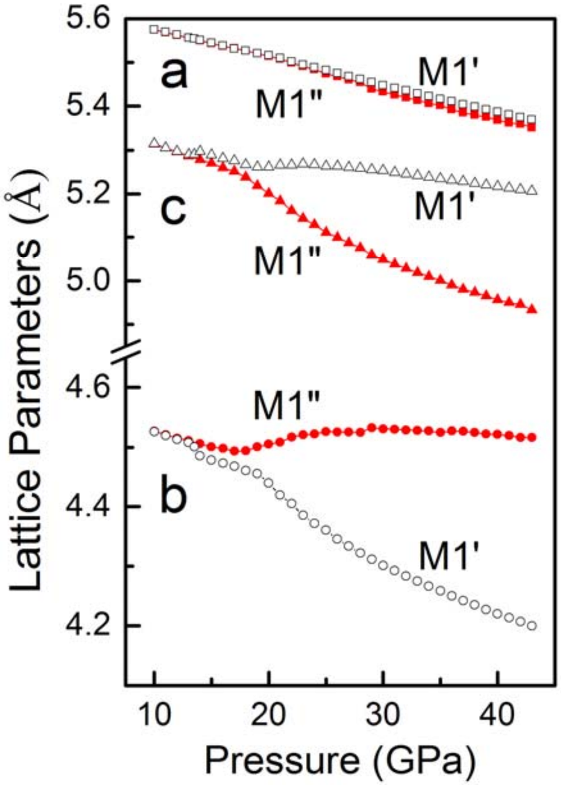

Figure 3. Lattice parameters of the M1’ and M1” phases under pressure showing the anisotropic compression behavior of both phases.

We would like to comment briefly on the energetics and relative stability of the M1’ and M1” phases. Our theoretical calculations suggest that these two phases are nearly degenerate, even after considering phonon contributions to the free energy. Thus current theory cannot make a decisive conclusion regarding the relative stability of these two phases. It appears that the M1’ phase is more stable experimentally. However, as we will discuss later, our electronic structure calculations strongly suggest that there should be a certain amount of M1” phase present in experimental samples.

C. Electronic structure of the M1’ and M1” phases and metallization mechanism

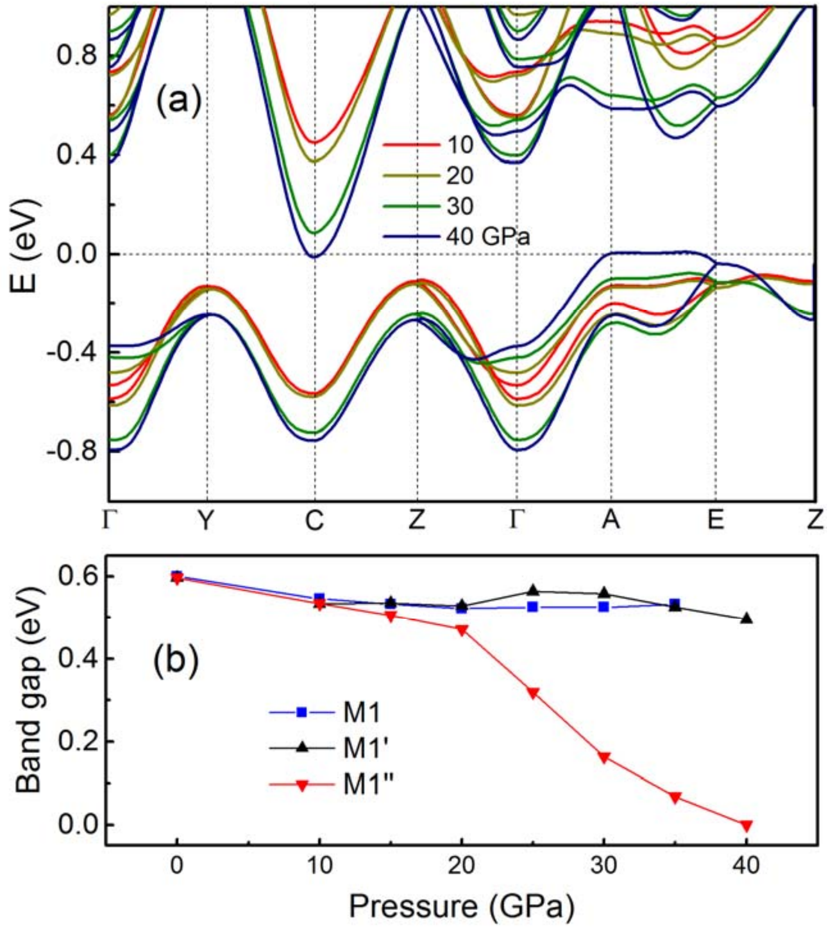

Figure 4. (a) Band structure of the M1" phase calculated at various pressures showing the significant pressure-dependent behavior. (b) Band gaps of the M1, M1' and M1" phases as functions of pressure.

As we have mentioned earlier, although the calculated lattice parameters of the M1' phase agree with the anisotropic compression behavior observed experimentally, earlier electronic structure study of the M1' phase did not seem to agree with the measured pressure-dependent resistivity [39, 40] which indicates a significant band gap reduction with increasing pressure. This discrepancy strongly suggests that other mechanisms must be responsible for the measured pressure-dependent resistivity, and the admixture of a certain amount of meta-stable phase such as the M1" phase discussed in previous sections is one such possible mechanism.

The electronic structure of the M1' and M1" phases under pressure are calculated using the DFT+U method with a *U* value of 2.65 eV. Figure 4(a) shows the band structure of the M1" phase calculated at various pressures. Unlike the M1' phase which shows a nearly pressure-independent gap (Figure 4(b)), the M1" phase shows a significant band gap reduction with increasing pressure at high pressures. The calculated band gap of the M1" phase starts to decrease quickly when pressure exceeds 20 GPa and the gap closes when the pressure reaches about 40 GPa. Experiments seem to suggest that the effective band gap (as measured by pressure-dependent resistivity) starts to decrease at lower pressures and the gap closes at around 30 GPa. [40]

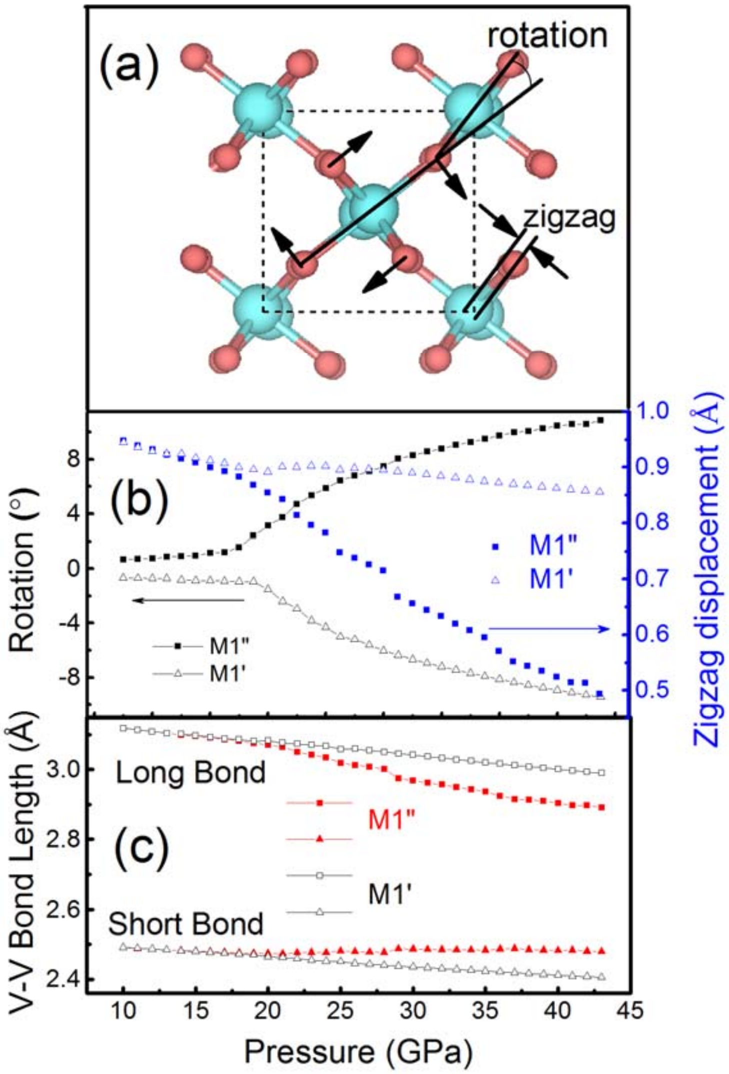

Figure 5. (a) Definitions of the rotation angle and zigzagging displacement of V atoms. (b) Rotation angle of the M1' and M1" phases under pressure. (c) V-V bond length of short and long bonds in M1' and M1" phases.

It should be pointed out that there may be multiple factors that contribute to the pressure-dependent resistivity. For example, defects (impurity) level may be strongly affected by pressure which may in turn affect the measured resistivity. Nevertheless, the observation of band gap closing at around 30 GPa [40] is rather convincing and our theoretical results for the M1" phase qualitatively agree with experiments. An overestimate for the metallization pressure is not surprising considering the limitation of current theory. Our results therefore strongly suggest that there might be some amount of the M1" phase present in experimental samples.

Since it is well known that the low energy electronic properties of VO_2 are dominated by the behavior of V *d* states, it is rather puzzling that opposite oxygen rotational distortions in the M1' and M1" phases can have such drastically different effects on the electronic properties. It is now generally agreed that the dimerization of the V atoms is critical for the development of an insulating gap in the M1 phase, but the gradual band gap closing clearly rules out a sudden breaking of V-V dimers as the mechanism for the pressure-induced metallization. It is possible, however, that a gradual reduction of the dimerization strength is responsible for the calculated pressure-dependent band gap of the M1" phase, and this reduction of dimerization strength should closely relate to the rotation of the oxygen octahedra discussed earlier.

To this end, we show in Figure 5 the evolution of relevant structural parameters (namely, rotation angle of oxygen octahedron, zigzagging displacement of V atoms, and the V-V bond lengths) of the M1' and M1" phases with pressure. The definitions of the rotation angle and the zigzagging displacement are shown schematically in Figure 5(a). Because of the clockwise rotation of the oxygen octahedron in the M1" phase, the V atoms along the chain direction are pulled towards forming a straight V chain at high pressure as shown in Figure 5(b). In other words, the zigzagging displacement of V atoms in the M1" phase is greatly suppressed as a result of the clockwise rotation of oxygen octahedron, and so is the V-V dimerization. This de-zigzagging in turn significantly reduces the energy of the conduction band, whereas the de-dimerization, measured by the difference between the long and short V-V bonds as shown in Figure 5(c), pushes the valence band up. These results are consistent with recent work concluding that the conduction bands (electron states) are primarily coupled with the zigzagging motion of V atoms whereas valence bands (hole states) are coupled with the V-V dimer vibration [11]. The de-zigzagging effects in the M1' phase are much weaker, and both the long and short V-V bonds vary linearly at the same rate with pressure.

Thus the pressure-induced band gap reduction in the M1" phases can be understood in terms of oxygen rotation induced de-dimerization and de-zigzagging of the V-V dimers. These results are consistent with current understanding of the role of Peierls dimerization in the development of an insulating gap in the monoclinic VO_2. Our results also provide a convincing explanation for the experimental observations.

IV. SUMMARY

Pressure-induced isostructural phase transition of monoclinic VO_2 and the underlying band gap reduction and metallization mechanisms are investigated using DFT based first-principles method. Phonon calculations reveal pressure-induced phonon softening in the M1 phase which ultimately leads to the isostructural phase transition. The phonon mode is found to be a $CaCl_2$-type of rotation of the oxygen octahedron. Rotational distortions restore the dynamical stability and give rise to the observed isostructural transition. We find that this phase transition is accompanied by an anisotropic compression, in excellent agreement with experiments. In addition to the experimentally identified M1' phase, we also predict a related M1" phase which is nearly degenerate with the M1' phase but could explain the experimentally observed pressure-induced band gap reduction and metallization of monoclinic VO_2. The rotation of the oxygen octahedron significantly alleviates but does not completely remove, the zigzagging and dimerization of V atoms in the M1" phase. This gradual de-dimerization and de-zigzagging mechanism are responsible for the observed band gap reduction of monoclinic VO_2 under high pressures.

ACKNOWLEDGEMENTS

This research was supported by the National Natural Science Foundation of China (Nos. 11274222, 11328401, 51672171 and 11628407), the National Key Basic Research Program of China (Grant No. 2015CB921600), the QiMingXing Project (Project No. 14QA1402000) of the Shanghai Municipal Science and Technology Commission, the Eastern Scholar Program, and the Shuguang Program (Grant No. 12SG34) from the Shanghai Municipal Education Commission. Special Program for Applied Research on Super Computation of the NSFC-Guangdong Joint Fund (the second phase), and Shanghai Supercomputer Center are also acknowledged. J. H. acknowledges the support from the Thousand Young Talents Program of China and the National Science Foundation of China (Grant No. 11572040). P. Z. is also supported by U.S. NSF under Grants DMR-1626967 and DMR-1506669.

REFERENCES

[1] Y. Li, S. Ji, Y. Gao, H. Luo, and M. Kanehira, Sci. Rep. **3**, 1370 (2013).

[2] Z. Zhang, Y. Gao, Z. Chen, J. Du, C. Cao, L. Kang, and H. Luo, Langmuir **26**, 10738 (2010).

[3] S. Cueff, D. Li, Y. Zhou, F. J. Wong, J. A. Kurvits, S. Ramanathan, and R. Zia, Nat Commun **6**, 8636 (2015).

[4] F. J. Morin, Phys. Rev. Lett. **3**, 34 (1959).

[5] B. Lazarovits, K. Kim, K. Haule, and G. Kotliar, Phys. Rev. B **81**, 115117 (2010).

[6] S. Kittiwatanakul, S. A. Wolf, and J. Lu, Appl. Phys. Lett. **105**, 073112 (2014).

[7] M. K. Liu *et al.*, Nature **487**, 345 (2012).

[8] B. Mayer *et al.*, Phys. Rev. B **91**, 235113 (2015).

[9] M. Nakano, K. Shibuya, D. Okuyama, T. Hatano, S. Ono, M. Kawasaki, Y. Iwasa, and Y. Tokura, Nature **487**, 459 (2012).

[10] J. Jeong, N. Aetukuri, T. Graf, T. D. Schladt, M. G. Samant, and S. S. Parkin, Science **339**, 1402 (2013).

[11] X. Yuan, W. Zhang, and P. Zhang, Phys. Rev. B **88**, 035119 (2013).

[12] S. Lysenko, A. Rúa, V. Vikhnin, F. Fernández, and H. Liu, Phys. Rev. B **76**, 035104 (2007).

[13] C. Kubler, H. Ehrke, R. Huber, R. Lopez, A. Halabica, R. F. Haglund, Jr., and A. Leitenstorfer, Phys. Rev. Lett. **99**, 116401 (2007).

[14] A. Cavalleri, C. Toth, C. W. Siders, J. A. Squier, F. Raksi, P. Forget, and J. C. Kieffer, Phys. Rev. Lett. **87**, 237401 (2001).

[15] P. Baum, D.-S. Yang, and A. H. Zewail, Science **318**, 788 (2007).

[16] T. L. Cocker, L. V. Titova, S. Fourmaux, G. Holloway, H. C. Bandulet, D. Brassard, J. C. Kieffer, M. A. El Khakani, and F. A. Hegmann, Phys. Rev. B **85**, 155120 (2012).

[17] A. Pashkin, C. Kübler, H. Ehrke, R. Lopez, A. Halabica, R. F. Haglund, R. Huber, and A.

Leitenstorfer, Phys. Rev. B **83**, 195120 (2011).

[18] M. Nakajima, N. Takubo, Z. Hiroi, Y. Ueda, and T. Suemoto, Appl. Phys. Lett. **92**, 011907 (2008).

[19] M. Huefner, R. K. Ghosh, E. Freeman, N. Shukla, H. Paik, D. G. Schlom, and S. Datta, Nano Lett. **14**, 6115 (2014).

[20] J. Laverock, S. Kittiwatanakul, A. A. Zakharov, Y. R. Niu, B. Chen, S. A. Wolf, J. W. Lu, and K. E. Smith, Phys. Rev. Lett. **113**, 216402 (2014).

[21] V. Eyert, Phys. Rev. Lett. **107**, 016401 (2011).

[22] J. M. Booth and P. S. Casey, Phys. Rev. Lett. **103**, 086402 (2009).

[23] S. Biermann, A. Poteryaev, A. I. Lichtenstein, and A. Georges, Phys. Rev. Lett. **94**, 026404 (2005).

[24] S. Chen, J. Liu, H. Luo, and Y. Gao, J. Phys. Chem. Lett **6**, 3650 (2015).

[25] J. B. Goodenough, J. Solid State Chem. **3**, 490 (1971).

[26] M. Gatti, F. Bruneval, V. Olevano, and L. Reining, Phys. Rev. Lett. **99**, 266402 (2007).

[27] M. M. Qazilbash *et al.*, Science **318**, 1750 (2007).

[28] J. B. Goodenough, Phys. Rev. **117**, 1442 (1960).

[29] D. Adler and H. Brooks, Phys. Rev. **155**, 826 (1967).

[30] R. M. Wentzcovitch, W. W. Schulz, and P. B. Allen, Phys. Rev. Lett. **72**, 3389 (1994).

[31] C. Weber, D. D. O'Regan, N. D. Hine, M. C. Payne, G. Kotliar, and P. B. Littlewood, Phys. Rev. Lett. **108**, 256402 (2012).

[32] X. Yuan, Y. Zhang, T. A. Abtew, P. Zhang, and W. Zhang, Phys. Rev. B **86**, 235103 (2012).

[33] N. B. Aetukuri *et al.*, Nat Phys **9**, 661 (2013).

[34] S. Kim, K. Kim, C. J. Kang, and B. I. Min, Phys. Rev. B **87**, 195106 (2013).

[35] J. D. Budai *et al.*, Nature **515**, 535 (2014).

[36] E. Arcangeletti, L. Baldassarre, D. Di Castro, S. Lupi, L. Malavasi, C. Marini, A. Perucchi, and P. Postorino, Phys. Rev. Lett. **98**, 196406 (2007).

[37] C. Marini, L. Baldassarre, M. Baldini, A. Perucchi, D. Di Castro, L. Malavasi, S. Lupi, and P. Postorino, High Pres. Res. **30**, 55 (2010).

[38] M. Mitrano, B. Maroni, C. Marini, M. Hanfland, B. Joseph, P. Postorino, and L. Malavasi, Phys. Rev. B **85**, 184108 (2012).

[39] X. Zhang *et al.*, RSC Adv. **5**, 54843 (2015).

[40] L. Bai, Q. Li, S. A. Corr, Y. Meng, C. Park, S. V. Sinogeikin, C. Ko, J. Wu, and G. Shen, Phys. Rev. B **91**, 104110 (2015).

[41] P. E. Blöchl, Phys. Rev. B **50**, 17953 (1994).

[42] G. Kresse and D. Joubert, Phys. Rev. B **59**, 1758 (1999).

[43] J. P. Perdew, K. Burke, and M. Ernzerhof, Phys. Rev. Lett. **77**, 3865 (1996).

[44] S. L. Dudarev, G. A. Botton, S. Y. Savrasov, C. J. Humphreys, and A. P. Sutton, Phys. Rev. B **57**, 1505 (1998).

[45] A. S. B. Hans W. Verleur, Jr., and C. N. Berglund, Phys. Rev. **172**, 788 (1968).

[46] B.-C. Shih, T. A. Abtew, X. Yuan, W. Zhang, and P. Zhang, Phys. Rev. B **86**, 165124 (2012).

[47] A. Togo, F. Oba, and I. Tanaka, Phys. Rev. B **78**, 134106 (2008).

[48] T. Miyake, P. Zhang, M. L. Cohen, and S. G. Louie, Phys. Rev. B **74**, 245213 (2006).

[49] B. C. Shih, Y. Xue, P. Zhang, M. L. Cohen, and S. G. Louie, Phys. Rev. Lett. **105**, 146401 (2010).

[50] T. Tohei, A. Kuwabara, T. Yamamoto, F. Oba, and I. Tanaka, Phys. Rev. Lett. **94**, 035502 (2005).

[51] R. Matzdorf, Z. Fang, Ismail, J. Zhang, T. Kimura, Y. Tokura, K. Terakura, and E. W. Plummer, Science **289**, 746 (2000).

[52] J. Haines and J. M. Léger, Phys. Rev. B **55**, 11144 (1997).